JOURNAL OF THE ROYAL SOCIETY Interface

In silico evolution of functional morphology: a test on bone tissue biomechanics

Emmanuel de Margerie, Paul Tafforeau and Lalaonirina Rakotomanana

J. R. Soc. Interface 2006 **3**, 679-687
doi: 10.1098/rsif.2006.0128

JOURNAL OF THE ROYAL SOCIETY Interface

J. R. Soc. Interface (2006) **3**, 679–687
doi:10.1098/rsif.2006.0128
Published online 4 May 2006

In silico evolution of functional morphology: a test on bone tissue biomechanics

Emmanuel de Margerie[1,2,*], Paul Tafforeau[3] and Lalaonirina Rakotomanana[1]

[1]*Institut de Recherche en Mathématiques de Rennes, CNRS UMR 6625, Campus Beaulieu, 35042 Rennes Cedex, France*
[2]*Comparative Osteohistology Group, CNRS FRE 2696, UPMC, MNHN, Collège de France, 2 place Jussieu, 75005 Paris, France*
[3]*European Synchrotron Radiation Facility, BP 220, 6 rue Jules Horowitz, 38046 Grenoble Cedex, France*

Evolutionary algorithms (EAs) use Darwinian principles—selection among random variation and heredity—to find solutions to complex problems. Mostly used in engineering, EAs gain growing interest in ecology and genetics. Here, we assess their usefulness in functional morphology, introducing finite element modelling (FEM) as a simulated mechanical environment for evaluating the 'fitness' of randomly varying structures. We used this method to identify biomechanical adaptations in bone tissue, a long-lasting problem in skeletal morphology. The algorithm started with a bone tissue model containing randomly distributed vascular spaces. The EA randomly mutated the distribution of vascular spaces, and selected the new structure if its mechanical resistance was increased. After some thousands of generations, organized phenotypes emerged, containing vascular canals and sinuses, mimicking real bone tissue organizations. This supported the hypothesis that natural bone microstructures can result from biomechanical adaptation. Despite its limited faithfulness to reality, we discuss the ability of the EA+FEM method to assess adaptation in a dynamic evolutionary framework, which is not possible in the real world because of the generation times of macro-organisms. We also point out the interesting potential of EAs to simulate not only adaptation, but also concurrent evolutionary phenomenons such as historical contingency.

Keywords: evolutionary algorithms; simulation; biomechanical adaptation; bone tissue; finite element modelling

1. INTRODUCTION

Evolutionary algorithms (EAs) are numeric optimization procedures inspired from Darwinian evolution (Goldberg 1989; Michalewicz 1992). Candidate solutions to a given problem are evaluated, selected, duplicated and randomly recombined and mutated, until an optimal (or satisfactory) solution is reached. These evolutionary computation techniques were proven to be powerful for solving complex problems, from structure engineering to molecular design (e.g. Deaven & Ho 1995; Willett 1995). EAs were also used to create and study artificial life-like systems in computers ('A-life'; e.g. Yedid & Bell 2001; Wilke & Adami 2002).

In conventional biology ('B-life'), though EAs took several years to get acceptance (Toquenaga & Wade 1996), they can provide a fully controllable Darwinian framework—selective pressure, mutation and recombination rates, as well as the genome structure of the individuals are set by the experimentator—inside which hypotheses about the evolutionary emergence of many biological patterns can be tested more easily than in the real world (Peck 2004). Consequently, EA simulations entered several biological disciplines, like ecology (Downing 1998; Sherratt & Roberts 1998; Cole 2002; Strand *et al.* 2002), genetics (Foster 2001; Quesneville & Anxolabéhère 2001; Behera & Nanjundiah 2004) and neurobiology (Rolls & Stringer 2000).

Our aim was to use EAs for studying the adaptive relationships between natural forms and their functions, i.e. functional morphology. Previous works applied EAs to morphological characters, but concerned artificial organisms: Sims (1994), aiming at creating realistic creatures in computer animations, simulated the emergence of articulated morphologies by testing their ability to walk, swim or jump in a virtual physical world. Interestingly, several adapted phenotypes recalled natural animal morphologies

*Author for correspondence (margerie.e.de@club.fr).

Received 2 March 2006
Accepted 29 March 2006

and locomotor modes. EAs were also used to make the morphology of robots evolvable (Lipson & Pollack 2000; Meyer & Guillot 2001). Still, a few studies suggest that EAs could also help to understand natural morphologies: simulations were tested on evolution of spider web shape (Krink & Vollrath 1997) and bone growth regulation (Nowlan & Prendergast 2005), for example. Though not based on an EA, Niklas (1994) also simulated 'phenotypic walks' of species (land plants) through complex morphospaces.

Here, we use an EA, coupled with finite element mechanical modelling (FEM), to test whether natural structures which have been proposed to be biomechanical adaptations (on the basis of comparative observations in a variety of species) (i) really provide mechanical advantage and (ii) would possibly emerge from a purely Darwinian process. Although question (i) might be more reliably assessed by an experimental approach (measuring *in vivo* or *in vitro* the biomechanical performance of a structure), addressing question (ii) is an attractive 'privilege' of EA simulations. Indeed, although an EA approach will probably remain an *in silico* simulation of limited faithfulness, it has the potential to test adaptive hypotheses in a truly evolutionary and dynamic framework: the emergence of an adaptive structure by selection can be observed throughout many generations. This is not feasible by experimental approaches in the real world, except for a few fast-generated organisms such as viruses or bacteria (e.g. Lenski & Travisano 1994).

The functional morphology problem we chosen as a test case is the possible biomechanical significance of bone micro-vascular organization: the geometrical arrangement of vascular canals within bone tissue has long been known to greatly vary between species and between long bones of the same skeleton (Foote 1916; Amprino & Godina 1947; Enlow & Brown 1958; de Ricqlès 1975). Several interpretations have been proposed in relation to various functions such as cell blood supply (Currey 1960) or bone growth dynamics (de Ricqlès 1975). Recently, quantitative morphometry on histological sections in bones of birds have suggested that vascular organization might have a biomechanical significance, i.e. the orientation of canals would be adapted to local stress modes (de Margerie 2002; de Margerie *et al.* 2005). Namely, whereas 'longitudinal' vascular canals (figure 1*a*) would be typical of axially loaded or bent long bones, a 'laminar' vascular network (figure 1*b*), predominantly found in some wing bones (humerus and ulna), could be an adaptation to torsional loads caused by flapping flight.

To test this hypothesis we simulated the optimization of the geometry of cavities within a solid, under several loading modes (axial or shear stresses). FEM was used to simulate loads on the solid and compute stress and strains in the structure. In other words, FEM provided the virtual environment in which fitness of structures generated by the EA could be measured.

2. MATERIAL AND METHODS

Simulations (both EA and FEM tests) were performed using Cast3M, a FEM software of the French Atomic Energy Agency (CEA), freely available for research at http://www-cast3m.cea.fr.

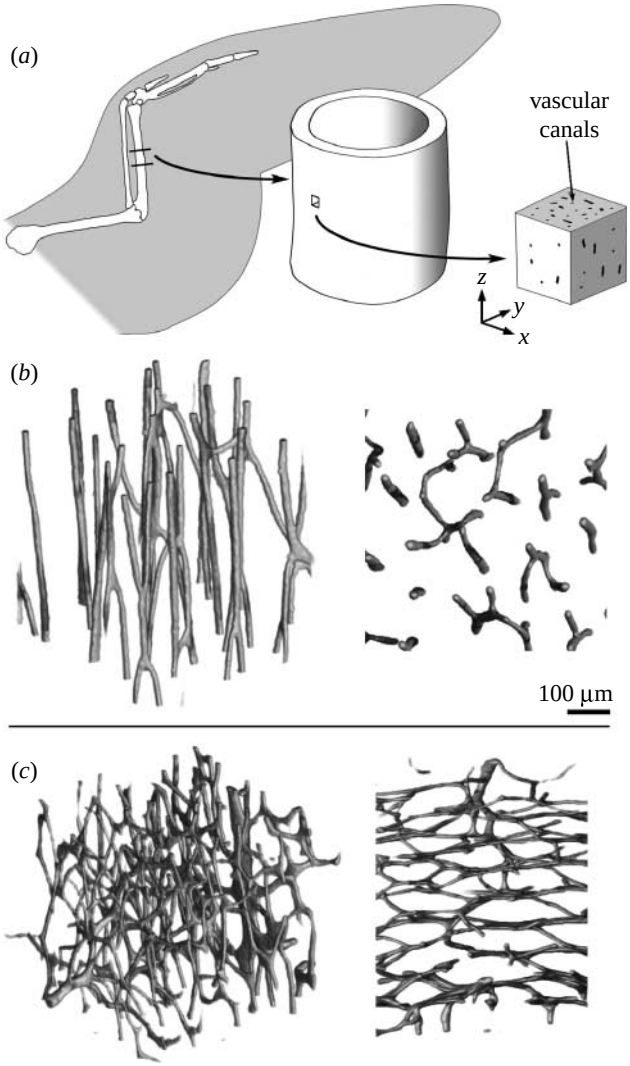

Figure 1. (*a*) Situation of bone samples. Vascular networks in real bone tissues: (*b*) longitudinal arrangement, usually found in bones resisting axial or bending loads (small fragment of the ulna of a white-chinned petrel; *Procellaria aequinoctialis*) and (*c*) laminar arrangement, observed in bones resisting torsional loads, e.g. wing long bones during flapping flight (ulna of a mallard; *Anas platyrhynchos*). Three-dimensional view on the left, cross-sectional view on the right. Renderings generated from phase contrast X-ray synchrotron microtomography, with a monochromatized beam at an energy of 30 keV, using a pixel size of 2.8 µm. The vascular network was extracted from the surrounding bone by three-dimensional segmentation using region growing (VGStudioMax 1.2).

2.1. Individuals

The phenotype of each 'individual' was a cubic block of bone tissue (figure 2*a*), comprising 1728 elements (12^3). Each element was $20\times20\times20$ µm, thus the whole cube had 0.24 mm edges and 0.138 mm^3 volume.

Elements were defined either bony or vascular (white and red in figure 2*a*, respectively). The ratio between the two types of elements assumed a 5% bone porosity, an usual value in real compact bone tissues (Cowin 2001). The number of vascular elements was thus 86,

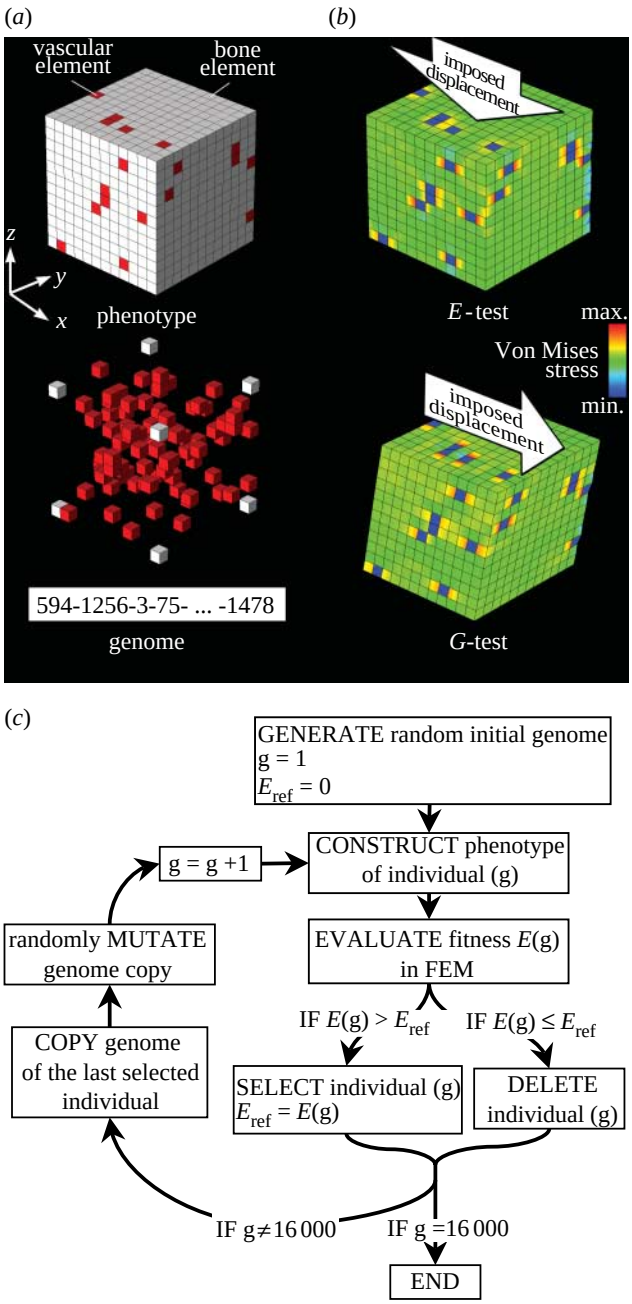

Figure 2. Simulation methods. (*a*) The distribution of vascular spaces within a model of bone tissue ('phenotype') was coded through a sequence of integers ('genome'). (*b*) The apparent stiffness of the tissue was measured in FEM, under pure compression (*E*-test, measuring Young's modulus *E*) or pure shear (*G*-test, measuring shear modulus *G*). Imposed displacements are exaggerated for clarity. (*c*) A simple EA using stiffness (either *E* or *G*) as a measure of 'fitness' was run for 16 000 'generations' to simulate bone tissue evolution.

scattered among 1642 bony elements (resulting porosity: 4.98%).

Position of vascular elements in the structure was coded through a sequence of 86 integers in the range 1–1728, each integer describing the position index of one vascular element (figure 2*a*). No particular ordering was imposed on the numbers in the sequence. On the other hand, repeats in the sequence were prevented throughout simulation, to preserve a constant porosity.

Each individual in the simulation was thus composed of a sequence (genome) and the associated tissue structure (phenotype).

2.2. FEM mechanical testing

To minimize the number of initial assumptions and to optimize the computation time, the mechanical model in FEM was assumed linear isotropic elastic. Bone elements were given a standard Young's modulus value $E_b = 20$ GPa. We assumed that vascular elements had a low contribution to the mechanical resistance of the tissue: their Young's modulus was set to $E_v = E_b/100 = 0.2$ GPa. Poisson ratio was set to 0.3 for all elements. Thus, the shear modulus of bony elements was $G_b = E_b/(2(1+0.3)) = 7.69$ GPa.

Individuals were tested either in pure compression (*E*-tests) or pure shear (*G*-tests). Preliminary tests showed that tension tests were unnecessary, since compression and tension loads yielded identical results according to linear elasticity. *E*-tests were thus representative of the local mechanical environment of a block of tissue situated in a bone shaft loaded either in pure compression, pure tension or bending (bending the whole bone shaft mainly causes compression on one side of the shaft and tension on the other side). On the other hand, *G*-tests simulated the condition of a small cube of tissue in a shaft undergoing pure torsion (twisting the whole bone shaft causes pure shear at the tissue level; Cowin 2001).

In *E*-tests (figure 2*b*), a 0.24 µm vertical (z) displacement was imposed on the cube upper face (equivalent to 1000 µstrain), while lower face vertical displacement was locked. Minimal additional constraints were added on lower edges to prevent lateral rigid translation of the cube. FEM calculated external forces needed to obtain these imposed displacements, as well as internal stresses, given the structure of the cube under investigation. The calculated vertical forces applied on the upper face were converted to a mean normal stress. The apparent stiffness modulus of the cube (Young's modulus, noted E, in Pa) was computed as the ratio between this stress and the imposed strain.

For *G*-tests (figure 2*b*), a 0.24 µm horizontal (x) displacement (1000 µstrain) was imposed on the upper face, while lower face x displacement and side faces z displacements were locked. Minimal additional constraints were added on lower edges to prevent translation of the cube. These boundary conditions were required to allow FEM resolution, and correctly simulated a pure shear small strain. After FEM resolution, the calculated forces in the x-direction on the upper face were converted to a mean tangential stress. This value was divided by the imposed angular strain to calculate the apparent shear modulus (noted G, in Pa) of the cube.

2.3. Evolution algorithm

Increasing the search speed and efficiency of original EAs has been the aim of much work (Goldberg 1989), producing plenty of methods and refinements available today. In the present work, we used a very simple

EA, minimizing assumptions and code complexity rather than maximizing search speed. Our EA used mutation and selection only (figure 2*c*). It started with a random structure (its genome was a sequence of random numbers). The phenotype of this first generation (g_1) individual was constructed and evaluated in a given mechanical environment, axial or torsional (through a E or G-test, respectively, in FEM). The apparent modulus was recorded as a measure of the individual's fitness. Then the genome was copied, producing a g_2 'child' individual, and subjected to one point mutation: one randomly determined integer among 86 was changed to a new random integer in the 1–1728 range. The mutation's phenotypic expression was thus a random displacement of one vascular element in the cube. The child structure was evaluated through the same mechanical test as its parent, returning a g_2 fitness value. At this point a selection was operated: if the g_2 fitness was greater than that in g_1, the child was selected and the parent was deleted. On the other hand, if the random mutation gave no mechanical advantage to the child, it was deleted and the parent was retained for further steps. Then the selected individual's genome (g_1 or g_2) was used to generate a g_3 genome, containing another punctual random mutation. The g_3 phenotype was evaluated and its fitness compared to its parent. The better resisting structure was selected and its genome copied and mutated to generate a g_4 individual, etc. Using only mutation (and no recombination) on single-individual generations (selection compares two consecutive generations), our algorithm imitates the simplest EAs (Rechenberg's EvolutionStrategie; Michalewicz 1992).

In each simulation, the algorithm was run for 16 000 generations. Computing time approached 16 h on an Intel Xeon BiProcessor computer. We performed three simulations using E-tests (axial stiffness optimization), using three different initial random structures. Starting with the same random structures, we performed three other simulations using G-tests (shear stiffness optimization).

3. RESULTS

3.1. Selection on axial stiffness

Evolution simulations using Young's modulus (E) as the selection criterion produced progressively more structured phenotypes (figure 3*a*). Starting from random positions of vascular elements at the initial generation ($g=1$), selection seemed to favour alignment of these elements in the z-direction, progressively constructing vascular columns of increasing length, somewhat analogous to longitudinal vascular canals (figure 1*a*). At $g=16\,000$, evolution resulted in strongly anisotropic structures, extended along the z-direction. No consistent anisotropy appeared in the transverse (x, y) plane, as illustrated on cross-sectional views of adapted phenotypes (figure 3*a*): structures roughly had transverse-isotropic symmetry.

The three runs of the algorithm, working on different random initial structures using different random mutations, produced three distinct adapted structures, but all presented a z-aligned anisotropy caused by more or less well-defined canals.

Fitness plots (figure 3*b*) show that stiffness increased similarly for all three simulations, although E values remained slightly different throughout the simulations.

On an absolute scale, E values evolved from 18.65 GPa at $g=1$ (mean value) to 18.96 GPa at $g=16\,000$, achieving a 1.7% increase on average. On a relative scale, given that pure bone has a 20 GPa modulus (E_b), the apparent modulus of the whole tissue (including vascular spaces) started its evolution at 93.3% of pure bone stiffness, and attained 94.8% after 16 000 generations. Thus, the stiffness 'cost' due to the 5% vascular porosity, which attained 1.35 GPa (6.7% of E_b) before optimization, was reduced to 1.04 GPa (5.2% E_b) by the EA. Consequently, the adaptive spatial arrangements of vascular cavities reduced the unfavourable mechanical effect of these cavities by 23%.

E increased much faster at the start of the simulation than later: plots had an asymptote around 19 GPa (which equals 95% E_b), illustrating that beneficial mutations happen less and less frequently with increasing structuring.

3.2. Selection on shear stiffness

Starting from the same initial random structures as previously, but using shear modulus (G) as the selection criterion, evolution produced phenotypes with a distinct type of structuring (figure 4*a*): vascular elements were progressively concentrated in (x, z) parallel planes. This arrangement was best observed in cross-sectional views, showing some analogy with laminar tissue pictures (figure 1*b*). Within these 'vascular planes', vascular elements did not form canals as in E runs but, rather, aligned along oblique directions and alternated with bone elements, constructing 'chessboard-like' structures. The structural anisotropy resulting from these (x, z) vascular planes was different from E runs: the adapted tissues in G runs were not transverse-isotropic.

Fitness plots (figure 4*b*) show that G increased by 1.4% during G runs, from 7.16 to 7.26 GPa (mean values). As previously, on a relative scale standardized on pure bone shear modulus G_b (7.69 GPa), evolution started near 93.1% of pure bone shear stiffness and ended around 94.4%. Thus, the stiffness cost due to vascular elements in the tissue is reduced from 0.53 GPa (6.9% G_b) to 0.43 GPa (5.6% G_b); the observed vascular arrangement reduced the mechanical cost of vascularity by 19%.

As for E runs, the three G runs followed very similar asymptotic paths and produced distinct but consistent adapted phenotypes: all three tissues exhibited some amount of (x, z) planar arrangement.

As additional 'controls' for the six runs, the shear stiffness (G) of each phenotype optimized for axial stiffness (E) was plotted in figure 4*b*, and vice versa in figure 3*b*. This revealed an unexpected pattern of balance between two adaptation criterions: optimizing axial stiffness only (E runs) generated phenotypes with

slightly decreased shear stiffness (−0.2% compared to initial random structures, on average; figure 4*b*), which suggested a trade-off (negative correlation) between E and G. However, adapting vascular structure to shear loads only (G runs) generated phenotypes with surprisingly increased axial stiffness, compared to initial random structures (+1.1% on average; figure 3*b*). This in turn suggested a positive correlation between E and G, at least along the evolutionary paths followed by G runs. In short, compared to random structures, longitudinal vascular canals increased axial stiffness but decreased shear stiffness. On the other hand, vascular planes increased both shear and axial stiffness.

A closer observation of stress and strain fields inside tissue structures allowed us to understand how canals and planes could increase the tissue mechanical resistance. They reduced stress concentrations that appeared locally around isolated vascular spaces (figure 2*b*). To measure this, the maximum local Von Mises shear stress within the tissue under load was noted at the start and at the end of each run. This showed that optimization of axial stiffness (E runs) came with a 26.0% decrease of maximal local stress (mean value of three runs). Similarly, optimization of shear stiffness (G runs) implied a 15.3% decrease of maximal local stress.

4. DISCUSSION

The 'proximate' aim of this study was to test whether natural vascular organizations might have a role in biomechanical performance of bone tissues, as comparative observations had suggested.

From adaptation simulations, it appeared that longitudinal vascular canals and parallel vascular planes might indeed represent structural optima for resisting axial and shear loads, respectively. FEM results gave details about how increased stiffness was provided: for their respective loading modes, vascular canals and planes reduced local stress concentrations and hence limited global strain amplitude for a given load. This showed that stiffness optimization also increases strength performance, since local stress concentration can cause microfractures and lead to bone failure (Cowin 2001). Which one of these features—more rigid bones or less fractures—has the most important effect on fitness of organisms in the real world remains an open question. Stiffer bones increase efficiency of locomotion by an improved transmission of muscular forces, hence reducing power requirements. Even a slight increase in stiffness might become significantly advantageous in the context of daily foraging or during migration, for which birds closely rely on an efficient use of body energy reserves. On the other hand, reducing fracture risk can obviously have a direct effect on fitness, because a broken bone would simply prevent foraging or migration, as well as increase predation risk, until bone healing is achieved. Though we cannot say which selective advantage is predominant (which probably depends on the locomotory habits of each species), it appears from FEM analysis that both stiffness and local stress reduction can simultaneously be optimized by geometrical arrangement of cavities in the tissue. While it is clear that, in our simulations, stiffness modulus has been used by the EA as a 'proxy' for stress reduction in bone tissue, it is possible that, in real species, natural selection has relied on both selective advantages (more efficient locomotion throughout daily locomotion, and less fracture accidents).

We note that the structuring of vascular spaces in canals and planes in compact bone tissues (5% porosity) recalls the 'rods and plates' arrangements of bone fraction in cancellous bone (porosity 80%), which are known to have an influence on the tissue mechanical properties (Cowin 2001) and have sometimes been considered as stress-mode specific arrangements in cancellous bone (van Rietbergen *et al.* 1996).

Here, we assumed that bone tissue structure has a genetic determinism and thus simulated its adaptation using a Darwinist algorithm. This approach is different from most previous work in the biomechanical field, which studied and simulated the structuring of bone tissue—compact or cancellous—as the result of external forces, through cell-mediated local remodelling during the life of the organism (e.g. van Rietbergen *et al.* 1996; Huiskes *et al.* 2000; Tsubota & Adachi 2004). This short time-scale remodelling (within weeks in compact bone; Terrier *et al.* 2005), sometimes called 'functional adaptation' (Carter *et al.* 1991), is popular in medical osteology, because it accounts for bone's impressive plasticity during the ontogenetic time. This epigenetic approach is in continuation of Wolff's 'Law of bone remodelling' (1892), and recalls D'Arcy Thompson's view of the role of external forces in skeletal morphology (Thompson 1917; Gould 2002). Though valuable in a physio-pathologic perspective, this approach does not account for the long time scale, hereditary origin of structures, nor for true Darwinian adaptation by natural selection, through geological time. Notably, structures constructed early in ontogeny, before locomotion comes in play, cannot reasonably depend on immediate external forces (Gould 2002, p. 1196). This applies to the present case, since primary vascular structure is set early in bird chicks (e.g. before the onset of flight in the mallard; Castanet *et al.* 1996). Our results showed that adapted bone tissue microstructure can emerge from a purely Darwinian mechanism (selection among random variation and heredity), and thus need not rely on short time-scale remodelling only.

Beyond pure morphology and the understanding of structural diversity, deciphering bone microstructure has noteworthy implications in medicine (prior to understanding bone pathologies, e.g. osteoporosis) and also in palaeobiology, using fossilized bone tissue as a proxy for biological traits of extinct species (e.g. de Ricqlès *et al.* 2000).

A more 'ultimate' aim for our study lies beyond bone biomechanics, and concerns the more theoretical, evolutionary implications of the simulation method itself.

We acknowledge that our basic morphological evolution model has several limitations. Most notably:

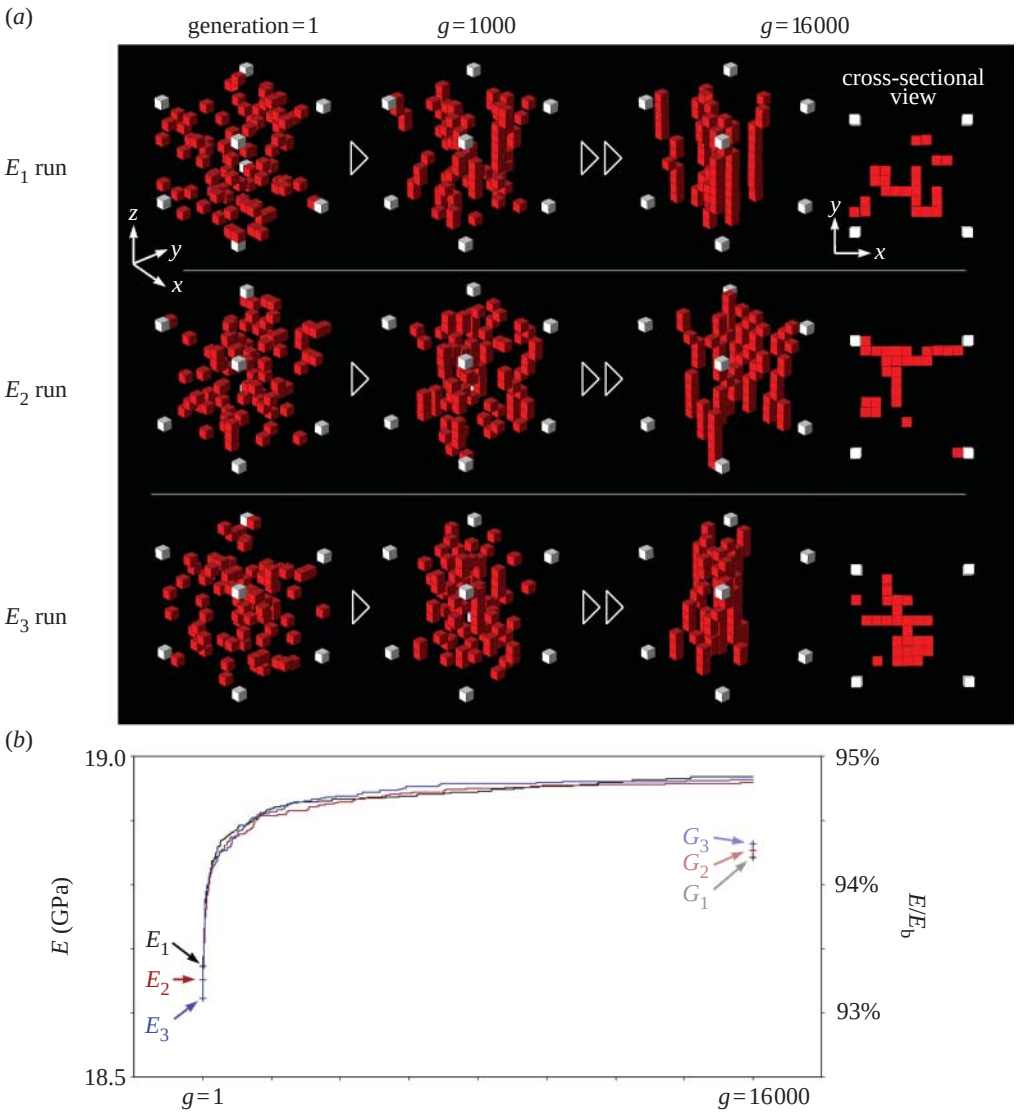

Figure 3. Evolution simulations using selection on axial stiffness. (*a*) Initial, intermediate and final phenotypes for three runs (E_1, E_2, E_3) of the EA. (*b*) Fitness plots throughout the evolution simulations (E_1, E_2, E_3). For comparison purpose, axial stiffness of structures optimized for shear stiffness (G_1, G_2, G_3, see figure 4) are also plotted.

(i) Ontogenesis of 'individuals' was trivial, since phenotype was directly and instantly deduced from genotype. Moreover, the genetic coding of the tissue structure was explicit (genome contained detailed positional information) which is probably unrealistic.

(ii) The phenotype definition was rather poor (12^3 elements), because larger phenotypes imply both longer FEM computation and larger search space for the EA (already 10^{147} possible phenotypes in the present configuration), causing unmanageably large computing times. Optimizing FEM resolution and EA search speed will thus be required for further work.

(iii) Our EA does not use recombination (i.e. crossover), an important operator in both natural and artificial evolution (Goldberg 1989). We preliminarily tested several EAs, including various amounts of recombination and mutation. We observed that including larger populations and recombination in the EA did not change the adapted patterns (canals and planes invariably emerged), nor improved search speed. Since we tried to avoid unnecessary complexity and arbitrariness in the setting of the EA parameters (population size and crossover rate must be set at some level), we preferred to retain the simpler EA for this first study, reflecting our desire to keep the model as simple as possible.

Clearly, the simplistic individual representations and evolutionary processes we used are unrealistic. Rather than reliably modelling the evolution and history of real bone tissues, our aim was to identify optimal structures using an optimization process based on Darwinian principles. In other words, our interest was to test whether any morphological adaptation can emerge from such an extreme distillation of biological evolution, from which remain only the minimal rules: random variation, selection and heredity.

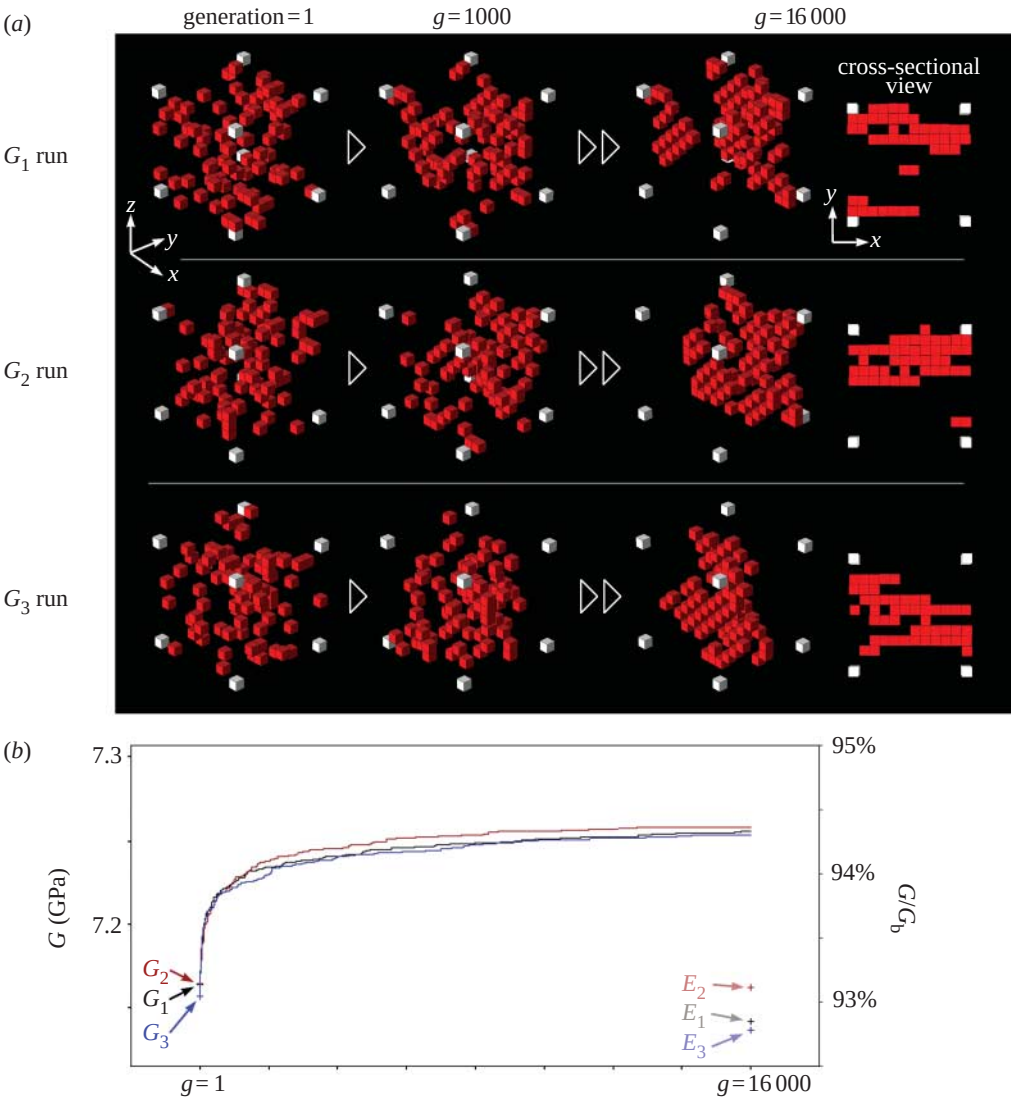

Figure 4. Evolution simulations using selection on shear stiffness. (*a*) Initial, intermediate and final phenotypes for three EA runs (G_1, G_2, G_3). (*b*) Fitness plots. For comparison purpose, shear stiffness of structures optimized for axial stiffness (E_1, E_2, E_3; see figure 3) are also plotted.

Despite the simplicity of our model, we observed that, starting from 'scratch' (unorganized random initial states), structured phenotypes emerged within some thousands of generations. Since our EA only involved duplication, random mutations and selection on stiffness modulus, we conclude that a simple stochastic exploration, only filtered by a selection on biomechanical performance, can easily generate organized structures. Accumulation of small changes produced well-organized structures at the end, evoking the continuum between micro- and macro-evolution (Gould 2002).

Changing the fitness criterion—from axial to shear stiffness—modified the structuring of the tissue. In other words, the EA was able to make the phenotype adapt to various mechanical environments, demonstrating an ability to generate structural diversity.

Moreover, some outcomes of the simulations suggest the potential usefulness of EAs to experiment on evolutionary concepts such as fitness landscape, evolutionary tempo, constraints, historical contingency or multi-task adaptation:

(i) The observed asymptotic path of our fitness variable through generations can be compared to results of experimental evolution. For example, Lenski & Travisano (1994) observed similar hyperbolic curves for cell size and fitness in bacterial populations placed in a static experimental environment. Such decelerating trajectories can reflect that the evolutionary path has reached a peak in the fitness landscape, and that more fit mutants appear less and less frequently, because 'major (fitness) improvements do not exist or else they are evolutionarily inaccessible' (Lenski & Travisano 1994). In our case, as adapted phenotypes (and genotypes) differ between each adaptation run (e.g. E_1, E_2, E_3), it appears that each run, because of its own starting point and experienced mutations, has found its way onto different fitness peaks in the landscape. These fitness peaks with very similar fitness levels (near 19 GPa for E runs) clearly correspond to each possible phenotype presenting vertical canals (or planes for G runs),

but at different places in the tissue. Hence, we can picture the fitness landscape of our simulations as containing a large number of approximately equivalent peaks. The relationship between the topology of the fitness landscape and the dynamics of adaptation (Niklas 1994) is an area of research where EAs could certainly be very helpful.

(ii) Before performing the simulations, we were concerned that, in the real world, connectivity of vascular spaces could be a constraint on the tissue evolution (because blood should circulate and reach all bone cells), which we did not implement in our model. Unexpectedly, connectivity of vascular elements emerged from scratch, constructing canals and sinuses under biomechanical selective pressures only. Hence, what we assumed as a constraint, limiting biomechanical evolution, might be a biomechanical adaptation itself. This is a basic example of how EAs can help to suggest hypotheses on what characters result from constraints or from adaptation.

(iii) In a virtual world, one can replicate evolution with identical selection criterions, but with different initial phenotypes (and different random mutations; e.g. E_1, E_2 and E_3), introducing some kind of contingency and historical or phylogenetic effects. This caused the EA to start from different places in the fitness landscape, and hence to reach different local optima: the three repeats produced distinct adaptations, which however resembled each other in their anisotropic organization, suggesting some degree of parallel evolution. 'Replicating history' (Lenski & Travisano 1994) may be one of the most valuable strengths of simulated (and experimental) evolution, for assessing the respective role of adaptation, phylogenetical constraints (by changing starting point) and chance (by changing mutations) in the emergence of a character.

(iv) We showed that an optimization of E implied a cost in G, but conversely an optimization of G increased E. This asymmetry in the relationship between E and G reveals that fitness landscapes for E and for G separately are parallel in some places and symmetrical in other places. In other words, some evolutionary paths in those landscapes lead to relative specialization (E runs), while other lead to versatility (G runs). A further step would be to include E and G simultaneously in the fitness function, to study multi-task adaptation to potentially conflicting functional requirements (Niklas 1994).

5. CONCLUSION

There is growing evidence in the literature that EAs are not only *in silico* avatars of Darwinian evolution, but seem to have high potentiality in various fields of real-world biology (e.g. Toquenaga & Wade 1996; Rolls & Stringer 2000; Foster 2001; Strand *et al.* 2002). Here we tested the extension of this potential to the field of functional morphology, by introducing FEM as an artificial mechanical environment. We observed that, although faithful simulations of organism morphology evolution might remain out of reach, simple simulations can already give valuable *analogical* arguments on pre-existing adaptive hypotheses, or even suggest new interpretations. Additionally, EAs appear to have abilities in more theoretical evolutionary biology (e.g. Behera & Nanjundiah 2004), as we could also deduce from our personal results.

Simulations have become a new kind of experimental system in a variety of sciences, including biology (Peck 2004). Whatever perspective is sought—applied or theoretical—simulations using EAs might provide a unique opportunity to overstep real-world time constraints and complexity, opening new ways to experiment on Darwinian adaptation and evolution.

We would like to thank N. Bideau, P. Eyi, G. Pichot and F. Razafimahery for their generous help on mechanical simulation.

REFERENCES

Amprino, R. & Godina, G. 1947 La struttura delle ossa nei vertebrati. *Com. Pont. Acad. Sci.* **9**, 329–463.

Behera, N. & Nanjundiah, V. 2004 Phenotypic plasticity can potentiate rapid evolutionary change. *J. Theor. Biol.* **226**, 177–184. (doi:10.1016/j.jtbi.2003.08.011)

Carter, D. R., Wong, M. & Orr, T. E. 1991 Musculoskeletal ontogeny, phylogeny, and functional adaptation. *J. Biomech.* **24**, 3–16. (doi:10.1016/0021-9290(91)90373-U)

Castanet, J., Grandin, A., Abourachid, A. & de Ricqlès, A. 1996 Expression de la dynamique de croissance osseuse dans la structure de l'os périostique chez *Anas platyrhynchos*. *CR Acad. Sci. III Vie* **319**, 301–308.

Cole, B. J. 2002 Evolution of self-organized systems. *Biol. Bull.* **202**, 256–261.

Cowin, S. C. 2001 *Bone mechanics handbook*. Boca Raton, FL: CRC Press.

Currey, J. D. 1960 Differences in the blood supply of bone of different histological types. *Q. J. Microsc. Sci.* **101**, 351–370.

de Margerie, E. 2002 Laminar bone as an adaptation to torsional loads in flapping flight. *J. Anat.* **201**, 521–526. (doi:10.1046/j.1469-7580.2002.00118.x)

de Margerie, E., Sanchez, S., Cubo, J. & Castanet, J. 2005 Torsional resistance as a principal component of the structural design of long bones: comparative multivariate evidence in birds. *Anat. Rec.* **282A**, 49–66.

de Ricqlès, A. 1975 Recherches paléohistologiques sur les os longs des Tétrapodes. VII: Sur la classification, la signification fonctionnelle et l'histoire des tissus osseux des Tétrapodes. *Ann. Paléont. (Vertébrés)* **61**, 51–129.

de Ricqlès, A., Padian, K., Horner, J. R. & Francillon-Vieillot, H. 2000 Palaeohistology of the bones of pterosaurs (Reptilia: Archosauria): anatomy, ontogeny, and biomechanical implications. *Zool. J. Linn. Soc.* **129**, 349–385. (doi:10.1006/zjls.1999.0239)

Deaven, D. M. & Ho, K. M. 1995 Molecular geometry optimization with a genetic algorithm. *Phys. Rev. Lett.* **75**, 288–291. (doi:10.1103/PhysRevLett.75.288)

Downing, K. 1998 Using evolutionary computational techniques in environmental modelling. *Environ. Model. Softw.* **13**, 519–528. (doi:10.1016/S1364-8152(98)00050-4)

Enlow, D. H. & Brown, S. O. 1958 A comparative histological study of fossil and recent bone tissues. Part III. *Tex. J. Sci.* **10**, 187–230.

Foote, J. S. 1916 A contribution to the comparative histology of the femur. *Smithson. Contrib. Knowl.* **35**, 1–242.

Foster, J. A. 2001 Computational genetics: evolutionary computation. *Nat. Rev. Genet.* **2**, 428–436. (doi:10.1038/35076523)

Goldberg, D. E. 1989 *Genetic algorithms in search, optimization, and machine learning*. Reading, MA: Addison-Wesley.

Gould, S. J. 2002 *The structure of evolutionary theory*. Cambridge, MA: Harvard University Press.

Huiskes, R., Ruimerman, R., van Lenthe, G. H. & Janssen, J. D. 2000 Effects of mechanical forces on maintenance and adaptation of form in trabecular bone. *Nature* **405**, 704–706. (doi:10.1038/35015116)

Krink, T. & Vollrath, F. 1997 Analysing spider web-building behavior with rule-based simulations and genetic algorithms. *J. Theor. Biol.* **185**, 321–331. (doi:10.1006/jtbi.1996.0306)

Lenski, E. R. & Travisano, M. 1994 Dynamics of adaptation and diversification: a 10,000-generation experiment with bacterial populations. *Proc. Natl Acad. Sci. USA* **91**, 6808–6814.

Lipson, H. & Pollack, J. B. 2000 Automatic design and manufacture of robotic lifeforms. *Nature* **406**, 974–978. (doi:10.1038/35023115)

Meyer, J. A. & Guillot, A. 2001 La robotique évolutionniste. *Pour La Science* **284**, 70–77.

Michalewicz, Z. 1992 *Genetic algorithms+data structures=evolution programs*. Berlin, Germany: Springer.

Niklas, K. J. 1994 Morphological evolution through complex domains of fitness. *Proc. Natl Acad. Sci. USA* **91**, 6772–6779.

Nowlan, N. C. & Prendergast, P. J. 2005 Evolution of mechanoregulation of bone growth will lead to non-optimal bone phenotypes. *J. Theor. Biol.* **235**, 408–418. (doi:10.1016/j.jtbi.2005.01.021)

Peck, S. L. 2004 Simulation as experiment: a philosophical reassessment for biological modeling. *Trends Ecol. Evol.* **19**, 530–534. (doi:10.1016/j.tree.2004.07.019)

Quesneville, H. & Anxolabéhère, D. 2001 Genetic algorithm-based model of evolutionary dynamics of class II transposable elements. *J. Theor. Biol.* **213**, 21–30. (doi:10.1006/jtbi.2001.2401)

Rolls, E. T. & Stringer, S. M. 2000 On the design of neural networks in the brain by genetic evolution. *Prog. Neurobiol.* **61**, 557–579. (doi:10.1016/S0301-0082(99)00066-0)

Sherratt, T. N. & Roberts, G. 1998 The evolution of generosity and choosiness in cooperative exchanges. *J. Theor. Biol.* **193**, 167–177. (doi:10.1006/jtbi.1998.0703)

Sims, K. 1994 Evolving virtual creatures. In *Computer Graphics, Annual Conf. Series (SIGGRAPH '94 Proc.)*, pp. 15–22.

Strand, E., Huse, G. & Giske, J. 2002 Artificial evolution of life history and behavior. *Am. Nat.* **159**, 624–644. (doi:10.1086/339997)

Terrier, A., Miyagaki, J., Fujie, H., Hayashi, K. & Rakotomanana, L. 2005 Delay of intracortical remodelling following a stress change: a theoretical and experimental study. *Clin. Biomech.* **20**, 998–1006.

Thompson, D'Arcy W. 1917 *On growth an form*. Cambridge, UK: Cambridge University Press.

Toquenaga, Y. & Wade, M. 1996 Sewall Wright meets artificial life: the origin and maintenance of evolutionary novelty. *Trends Ecol. Evol.* **11**, 478–482. (doi:10.1016/0169-5347(96)20075-8)

Tsubota, K. & Adachi, T. 2004 Changes in the fabric and compliance tensors of cancellous bone due to trabecular surface remodeling, predicted by a digital image-based model. *Comp. Meth. Biomech. Biomed. Eng.* **7**, 187–192. (doi:10.1080/10255840410001729524)

van Rietbergen, B., Mullender, M. G. & Huiskes, R. 1996 A three dimensional model for osteocyte-regulated remodeling simulation at the tissue level. In *Computer methods in biomechanics & biomedical engineering* (ed. J. Middleton, M. L. Jones & G. N. Pande). London, UK: Gordon & Breach.

Wilke, C. O. & Adami, C. 2002 The biology of digital organisms. *Trends Ecol. Evol.* **17**, 528–532. (doi:10.1016/S0169-5347(02)02612-5)

Willett, P. 1995 Genetic algorithms in molecular recognition and design. *Tibtech* **13**, 516–521.

Wolff, J. 1892 *Das Gesetz der Transformation der Knochen*. Berlin, Germany: A. Hirshwald Verlag.

Yedid, G. & Bell, G. 2001 Microevolution in an electronic microcosm. *Am. Nat.* **157**, 465–486. (doi:10.1086/319928)